The Effect of Temperature on the Frequency Response of p-i-n Photodiodes for Optical Communications

Jorge Manuel Torres Pereira
Instituto de Telecomunicações, Av. Rovisco Pais 1, 1049-001 Lisboa, Portugal
Phone: +351-218417289, Fax: +351-218417672, e-mail: torres.pereira@lx.it.pt

***Abstract* — The effect of temperature on the transit time limited frequency response of p-i-n photodiodes is investigated. The temperature effects are embodied in the absorption coefficient, in the electron and hole mobilities and in the electron and hole saturation drift velocities. The numerical model is applied to devices with a linear electric field profile in the absorption region and non-uniform illumination. The results show, for a given reverse bias voltage, that the bandwidth decreases when the temperature increases.**

I. Introduction

Photodiodes are key devices for optical communication systems due to their good frequency response and easy of fabrication. The basic diode structure is a double heterojunction of the p-i-n type. These p-i-n photodiodes are known to have lower dark current and noise than those based on homojunctions. For long wavelength operation, 1.0 – 1.6 μm, the p and n regions are of InP and the lightly doped i region is of the lattice matched ternary semiconductor $In_{0.53}Ga_{0.47}As$ [1].

The photodiode's frequency response may determine the optical communication systems' performance and therefore it is important to have a detailed knowledge of its behavior. Several approaches have been used to obtain the frequency response of p-i-n photodiodes [2-4]. A simple and very general numerical technique, which removes some of the limitations of those models, made possible the study of the structural, bias voltage and illumination effects on the frequency response of avalanche and p-i-n photodiodes [5-8]. This numerical technique is used to investigate the effects of temperature on the frequency response of p-i-n photodiodes.

II. Device Structure and Modeling

A. Device Structure

The schematic of the p-i-n structure under study is shown in Fig. 1. The contact layers are of n and p highly doped InP semiconductor. The absorption layer is assumed to be of n lightly doped $In_{0.53}Ga_{0.47}As$. The incident light is assumed to be incident on the p side and is absorbed only in the ternary semiconductor layer. The photogenerated carriers are driven to the contacts by the electric field which is supposed to extend through the entire absorption region. This condition may be obtained by an adequate reverse bias voltage.

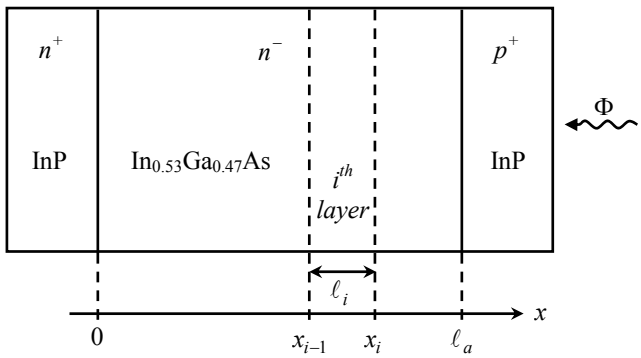

Fig. 1. The p-i-n structure under study. The light is incident on the p side.

B. Numerical Model

The implemented numerical model starts by dividing the absorption region into any desired number of layers and the continuity equations are solved, for each layer, assuming that within the layer the carriers' drift velocities are constant. The frequency response of the multilayer structure is then calculated from the response of each layer using matrix algebra. This model may be applied to any electric field profile in the absorption region, the accuracy depending on the number and size of layers.

In the frequency domain the electron and hole current densities in the ith layer, $J_{in}(x,\omega)$ and $J_{ip}(x,\omega)$, respectively, obey the following equations [5]:

$$\frac{i\omega}{v_{in}} J_{in}(x,\omega) = \frac{d\,J_{in}(x,\omega)}{dx} + G_i(x,\omega) \qquad (1)$$

$$\frac{i\omega}{v_{ip}} J_{ip}(x,\omega) = -\frac{d\,J_{ip}(x,\omega)}{dx} + G_i(x,\omega) \qquad (2)$$

where v_{in}, v_{ip} are the electron and hole drift velocities respectively and $G_i(x,\omega)$ refers to the electron-hole optical generation rate given by

$$G_i(x,\omega) = q\,\alpha\phi_1\, e^{-\alpha(\ell_a - x)} \quad \left(x_{i-1} \le x \le x_i\right) \qquad (3)$$

This work was sponsored by Instituto deTelecomunicações, pólo de Lisboa.

The parameter α is the absorption coefficient, q is the magnitude of the electron charge and ϕ_1 is the amplitude of the sinusoidal input optical flux component.

By solving the continuity equations (1) and (2), the ith layer may then be represented by a set of linear response coefficients $T_i, \vec{S}_i, \vec{R}_i$ and D_i. The quantities $T_i, \vec{S}_i$ are related to the electron and hole current densities through the equations

$$\begin{bmatrix} J_p(x_i) \\ J_n(x_i) \end{bmatrix} = T_i \begin{bmatrix} J_p(x_{i-1}) \\ J_n(x_{i-1}) \end{bmatrix} + \vec{S}_i \tag{4}$$

with

$$T_i = \begin{bmatrix} T_{ipp} & T_{ipn} \\ T_{inp} & T_{inn} \end{bmatrix} \quad and \quad \vec{S}_i = \begin{bmatrix} S_{ip} \\ S_{in} \end{bmatrix}. \tag{5}$$

The quantities $\vec{R}_i$ and D_i are obtained from the equation

$$p_i(\omega) = \vec{R}_i^T \begin{bmatrix} J_p(x_{i-1}) \\ J_n(x_{i-1}) \end{bmatrix} + D_i \tag{6}$$

where

$$p_i(\omega) = \int_{\ell_i} \left[J_n(x,\omega) + J_p(x,\omega) \right] dx . \tag{7}$$

The quantity D_i is a scalar whereas $\vec{R}_i^T = \begin{bmatrix} R_{ip} & R_{in} \end{bmatrix}$.

The four linear response coefficients may be used now to compute the corresponding response coefficients of the multilayer structure by following a simple set of rules:

$$\begin{aligned} T_{i+1,i} &= T_{i+1} T_i \\ \vec{S}_{i+1,i} &= \vec{S}_{i+1} + T_{i+1} \vec{S}_i \\ \vec{R}_{i+1,i}^T &= \vec{R}_{i+1}^T T_i + \vec{R}_i^T \\ D_{i+1,i} &= \vec{R}_{i+1}^T \vec{S}_i + D_{i+1} + D_i \end{aligned} \tag{8}$$

where subscripts (i), (i+1) and (i+1,i) refer to the ith layer, (i+1)th layer and the union of the two layers respectively.

The frequency response is obtained from

$$I(\omega) = \delta(\omega)/\ell_a \tag{9}$$

where the response scalar $\delta(\omega)$ is given by

$$\delta(\omega) = D - R_n S_n / T_{nn} . \tag{10}$$

The quantities D, R_n, S_n, T_{nn}, for the multilayer structure, are obtained by repeated application of (8).

Solving (1) and (2) using (3) and relating the current densities as in (4) we are able to obtain T_i and $\vec{S}_i$:

$$T_i = \begin{bmatrix} e^{-i\omega\tau_{ip}} & 0 \\ 0 & e^{i\omega\tau_{in}} \end{bmatrix} \tag{11}$$

$$\vec{S}_i = q\alpha\phi_1 \ell_i \quad e^{-\alpha(\ell_a - x_i)} \begin{bmatrix} f\left(i\omega\tau_{ip} + \alpha\ell_i\right) \\ -f\left(-i\omega\tau_{in} + \alpha\ell_i\right) \end{bmatrix} \tag{12}$$

with $\tau_{ip} = \ell_i / \mathrm{v}_{ip}, \tau_{in} = \ell_i / \mathrm{v}_{in}$ and $f(\theta) = (1 - e^{-\theta})/\theta$.

The quantities $\vec{R}_i$ and D_i are obtained from (6) taking into account (7):

$$\vec{R}_i = \ell_i \begin{bmatrix} f\left(i\omega\tau_{ip}\right) \\ f\left(-i\omega\tau_{in}\right) \end{bmatrix} \tag{13}$$

$$D_i = q\alpha\phi_1 \ell_i^2 e^{-\alpha\ell_a} e^{-\alpha(\ell_i - x_i)} \left[\frac{f\left(-\alpha\ell_i\right) - f\left(-i\omega\tau_{in}\right)}{-\alpha\ell_i + i\omega\tau_{in}} + \frac{f\left(-\alpha\ell_i\right) - f\left(i\omega\tau_{ip}\right)}{\alpha\ell_i + i\omega\tau_{ip}} \right] \tag{14}$$

In this work a linear electric field profile is assumed and may be expressed as [9],

$$E(x) = \frac{2U_d}{\ell_a^2} x + \left(\frac{U - U_d}{\ell_a} \right) \qquad (U > U_d) \tag{15}$$

with $U_d = \dfrac{qN_d \ell_a^2}{2\varepsilon_n}$. U_d is called the punchthrough voltage, U is the reverse bias voltage, N_d is the residual donor concentration in the absorption region and ε_n is the InGaAs dielectric constant. By dividing the absorption region into a certain number of layers enables us to assign to each layer a constant value for the electric field. These discrete values of the electric field are then used to obtain the carriers' drift velocities in each layer where they are assumed to be constant. The electron and hole drift velocities in the InGaAs are calculated, for each value of the electric field, from two empirical expressions that show very good agreement with experimental results [3]:

$$\begin{aligned} \mathrm{v}_n(E) &= \left(\mu_n E + \beta \mathrm{v}_{n\ell} E^\gamma\right) / \left(1 + \beta E^\gamma\right) \\ \mathrm{v}_p(E) &= \mathrm{v}_{p\ell} \tanh\left(\mu_p E / \mathrm{v}_{p\ell}\right) \end{aligned} \tag{16}$$

where μ_n and μ_p are the electron and hole mobilities, $\mathrm{v}_{n\ell}$ and $\mathrm{v}_{p\ell}$ are the electron and hole saturation velocities and β and γ are adjusting constants, β =7.4x10^{-15} (m/V)$^{2.5}$; γ =2.5 .

The temperature affects the drift velocities because the mobilities and the saturation velocities change with temperature. For the InGaAs we assume that, for the range of temperatures under consideration, $\mu \propto T^{-1}$ [10] and that the saturation drift velocities may be expressed as [11]

$$\begin{aligned} \mathrm{v}_{n\ell} &= 7.7\mathrm{x}10^4 - 53T \qquad (m/s) \\ \mathrm{v}_{p\ell} &= 6.59\mathrm{x}10^4 - 53.4T \quad (m/s) \end{aligned} \tag{17}$$

The electron and hole drift velocities, as a function of the electric field for T= 300K and T= 350K, are shown in Fig. 2.

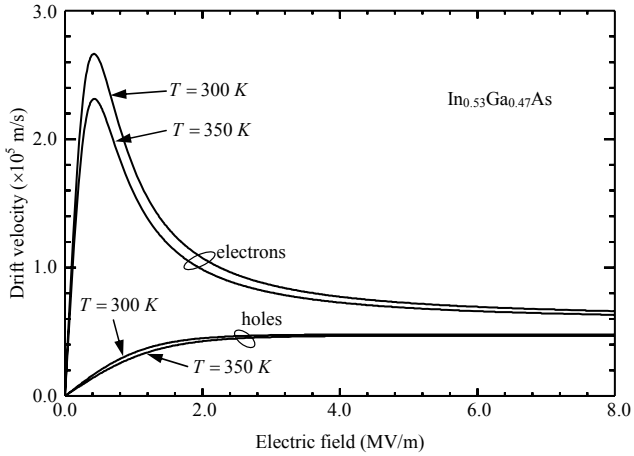

Fig. 2. Drift velocities for electrons and holes at T= 300 K and T= 350 K.

The absorption coefficient depends on temperature mainly due to changes in the energy band gap, W_G. For $In_{0.53}Ga_{0.47}As$ it may be expressed as

$$\alpha(T) = \alpha(300)\sqrt{\frac{hf - W_G(T)}{hf - W_G(300)}} \tag{18}$$

with [12]

$$W_G(T) = 0.812 - 3.26\text{x}10^{-4}T + \\ + 3.31\text{x}10^{-7}T^2 \quad (eV) \tag{19}$$

where h is the Planck's constant and f is the frequency of the incident optical radiation.

III. Results and Discussion

A list of the material parameters, used in the numerical simulations, is presented in Table I.

Table I
Material parameters at 300 K

Parameter	Units	$In_{0.53}Ga_{0.47}As$
α (λ=1.3 μm)	m^{-1}	1.15×10^6
W_G	eV	0.744
ε_n	F/m	14.1 ε_0
μ_n	$m^2V^{-1}s^{-1}$	1.05
μ_p	$m^2V^{-1}s^{-1}$	0.042
v_{nl}	m/s	$6\text{x}10^4$
v_{pl}	m/s	$4.8\text{x}10^4$

In the calculations it was assumed a residual donor concentration $N_d = 10^{21} m^{-3}$ and a reverse bias voltage of 6 V and 10 V. The temperature was set at 273 K, 300 K and 350 K. The number of layers was fixed at 100 although a lower number of layers may have been used without loss of accuracy [13].

Fig.3 shows the frequency response of two structures, $\ell_a = 1.5\mu m$ and $\ell_a = 3\mu m$, at temperatures T=273, 300 and 350 K, for U= 10 V. For the same width of the absorption region it is seen that the photodiode has a better frequency response at lower temperatures. These results may be explained considering that the temperature affects more the drift velocity than the absorption coefficient [2]. Shorter devices, as expected, respond better and seem to be less sensitive to temperature than longer devices.

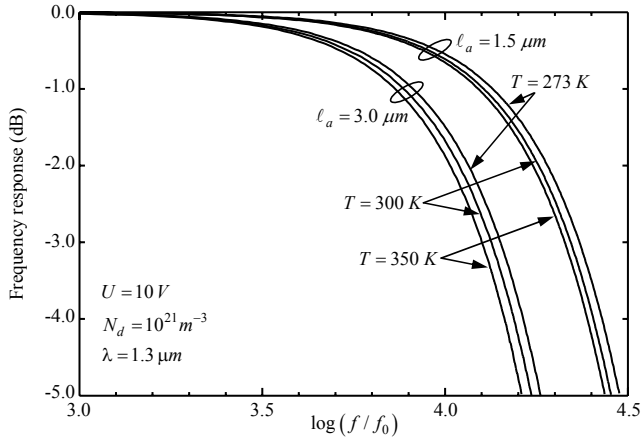

Fig. 3. Frequency response of the p-i-n photodiode for U= 10 V; ℓ_a = 1.5μm and 3 μm; T=273, 300 and 350 K (f_0= 1 MHz).

The frequency response of a photodiode with $\ell_a = 3\mu m$, U= 6 and 10 V , T= 273 and 350 K, is shown in Fig. 4. For a fixed temperature the frequency response is better when the bias voltage is 6 V. This may be due to the fact that, being the light incident on the p side, the photogenerated electrons are the dominant carriers and therefore lower electric fields may be responsible for higher drift velocities, Fig. 2. The frequency response seems to be more sensitive to temperature for lower bias voltage which is also explained in terms of the drift velocity- electric field curves shown in Fig. 2.

Fig. 5 shows the 3-dB bandwidth of p-i-n photodiodes as a function of the absorption region width for U= 6 and 10 V, T= 273 and 350 K. At a fixed temperature a better bandwidth is obtained for lower bias voltage which may be due to the velocity-field type of dependence for the electrons and the electric field profile in the absorption region. The effect of temperature is also more important for smaller values of the reverse bias voltage because for lower values of the electric field the drift velocities are more sensitive to temperature. For a temperature increase from 273 to 350 K the bandwidth is seen to decrease more than 2 GHz when U= 6 V.

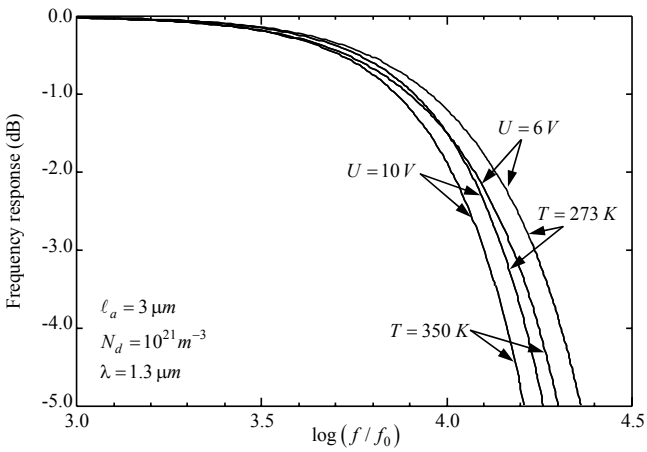

Fig. 4. Frequency response of the p-i-n photodiode with ℓ_a = 3μm ; U= 6 and 10 V; T=273 and 350 K (f_0= 1 MHz)..

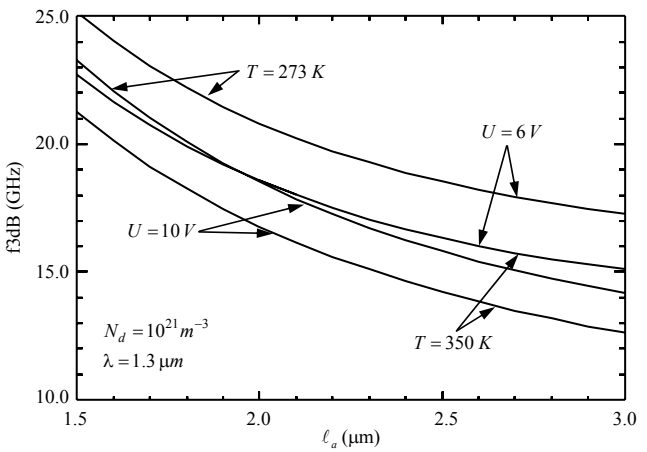

Fig. 5. The 3-dB bandwidth as a function of the absorption region width for *U*= 6 and 10 V at 273 K and 350 K.

IV. CONCLUSIONS

This paper investigates the effect of temperature on the frequency response of p-i-n photodiodes of the type InP/InGaAs/InP. The numerical model assumes that the absorption region is divided into a certain number of layers, each one represented by a set of linear response coefficients. The frequency response of the multilayer structure is then calculated from the response of each layer using matrix algebra. The effect of temperature on the device's frequency response was related to the temperature dependence of the carriers' drift velocity and the absorption coefficient. An increase of temperature is seen to decrease the drift velocity and increase the absorption coefficient. The results show a decrease of the photodiode's bandwidth when the temperature increases which means that the frequency response is determined by the effect of temperature on the drift velocities. It is also seen that the device's bandwidth is more sensitive to temperature for lower reverse bias voltage which may be explained in terms of the velocity–field type of dependence and also of the electric field profile in the absorption region.

REFERENCES

[1] G.E. Stillman, L.W. Cook, N.Tabatabaie, G.E. Bulman, V.M. Robbins "InGaAsP photodiodes", *IEEE Trans. Electron Devices,* vol. ED-30, pp. 364-381, April 1983.

[2] G. Lucovsky, R.F. Schwarz, R.B. Emmons, "Transit-time considerations in p-i-n diodes", *J. Appl. Phys*., vol.35, nº3, pp. 622-628, 1964.

[3] M. Dentan, B. de Cremoux, "Numerical simulation of the nonlinear response of a p-i-n photodiode under high illumination", *J. Lightwave Technol.*, vol. 8, nº 8, pp.1137-1144, August 1990.

[4] J. Harari, G. Jin, J.P. Vilcot, D. Decoster, "Theoretical study of p-i-n photodetectors' power limitations from 2.5 to 60 GHz", *IEEE Trans. Microwave Theory Tech*, vol. 45 nº 8, pp.1332-1336, August 1997.

[5] J.N. Hollenhorst, "Frequency response theory for multilayer photodiodes", *J. Lightwave Technol.*, vol.8, nº4, pp.531-537, 1990.

[6] J.M. Torres Pereira, "Frequency response simulation analysis of InGaAsP/InP SAM-APD devices", *Microwave Opt. Technol. Lett.*, vol. 48, nº4, pp. 712-717, April 2006.

[7] J.M. Torres Pereira, "Modeling the frequency response of p^+InP/n^-InGaAs/n^+InP photodiodes with an arbitrary electric field profile", *COMPEL - The International Journal for Computation and Mathematics in Electrical and Electronic Engineering*, Vol. 26, nº 4, pp. 1114-1122, 2007.

[8] J.M. Torres Pereira, "The effect of the direction of incident light on the frequency response of p-i-n photodiodes" in *Studies in Appl. Electromagnetics and Mechanics 30 - Advanced Computer Techniques in Applied Electromagnetics*, S. Wiak et als. (Eds.) IOS Press 2008, pp. 417-424.

[9] J.B. Radunovic, D.M. Gvozdic, "Nonstationary and nonlinear response of a p-i-n photodiode made of two-valley semiconductor", *IEEE Trans. Electron Devices*, vol. 40 nº 7, pp.1238-1244, July 1993.

[10] S. Adachi, *Physical Properties of III-V Semiconductor Compounds*, Wiley, 1992, pp. 223-238.

[11] S. Adachi, *Physical Properties of III-V Semiconductor Compounds*, Wiley, 1992, pp. 246-247.

[12] T. P. Pearsall, "$Ga_{0.47}In_{0.53}As$: A Ternary Semiconductor for Photodetector Applications", *IEEE J. Quantum Electron.,* vol. QE-16, pp. 709-719, July 1980.

[13] J.M. Torres Pereira ,"Frequency Response Analysis of InGaAs/InP Photodiodes", in *Proceedings of Conftele2007 - 6th Conference on Telecommunications*, Peniche, Portugal, May 2007, pp. 287-290.